Environmental Science & Technology

Article

Cite This: Environ. Sci. Technol. 2018, 52, 8745−8755

pubs.acs.org/est

Silver Toxicity Thresholds for Multiple Soil Microbial Biomarkers

Sotirios Vasileiadis,[†,‡] Gianluca Brunetti,[†] Ezzat Marzouk,[†,§] Steven Wakelin,[∥] George A Kowalchuk,[⊥] Enzo Lombi,[†] and Erica Donner*[,†]

[†]Future Industries Institute, University of South Australia, Mawson Lakes 5095, Australia

[‡]Department of Biochemistry and Biotechnology, University of Thessaly, Biopolis 41500, Larissa, Greece

[§]Division of Soil and Water Sciences, Arish University, Dahyet El Salam, El Arish, North Sinai, 31111, Egypt

[∥]Scion Research, Christchurch 8011, New Zealand

[⊥]Institute of Environmental Biology, Utrecht University, Utrecht 3584 CH, The Netherlands

Supporting Information

ABSTRACT: Material flow analysis shows that soil is a key repository for silver (Ag) from (nano)silver-functionalized consumer products, but the potential effects of Ag toxicity, via Ag^+ release, on soil microbial communities and their ecosystem services remains largely unknown. We examined the responses of multiple microbial biomarkers to increasing Ag^+ doses (nine concentrations, 0−2000 mg kg^{-1}) in nine different soils representing a wide range of soil properties. Analyses included substrate-induced microbial respiration, nine different soil enzyme activities, and quantification of bacterial 16S-rRNA (SSU) and fungal intergenic spacer (ITS) copies. The resulting half-maximal effective concentrations (EC_{50}) for Ag ranged from ∼1 to >500 mg kg^{-1} and showed soil-specific responses, including some hormesis-type responses. Carbon cycle-associated enzyme activities (e.g., cellobiohydrolase, xylosidase, and α/β-glucosidase) responded similarly to Ag. Sulfatase and leucine−aminopeptidase activities (linked to the sulfur and nitrogen cycles) were the most sensitive to Ag. Total organic carbon, and to a lesser extent pH, were identified as potentially useful response predictors, but only for some biomarkers; this reflects the complexity of soil Ag chemistry. Our results show Ag toxicity is highly dependent on soil characteristics and the specific microbial parameter under investigation, but end point redundancies also indicated that representative parameters for key microbial functions can be identified for risk assessment purposes. Sulfatase activity may be an important Ag toxicity biomarker; its response was highly sensitive and not correlated with that of other biomarkers.

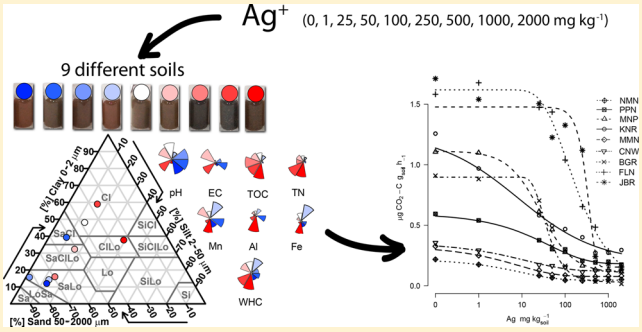

INTRODUCTION

Silver (Ag) has potent antimicrobial properties and is used for this function in a wide variety of commercial products, ranging from biomedical products (antiseptic dressings, catheters, and prostheses) to personal care products, textiles, and paints.[1−3] Widespread industrial and commercial use of Ag-containing products is apparent in the nanoproduct inventories and databases curated by credible specialist organisations,[4,5] and results in the release of Ag into the environment via the municipal wastewater → sludge/biosolids → soil exposure pathway.[6,7]

The chemistry of Ag in soil is complex. Over time, ionic Ag (Ag^+) transforms to less soluble forms such as metallic Ag (Ag^0), Ag sulfide (Ag_2S), and AgCl compounds.[8−11] Through the wastewater−biosolids pathway, Ag most likely reaches soil predominantly as Ag_2S (e.g., Kaegi et al.[12]), but other minor Ag species may also be present,[13] and the long-term stability and solubility of Ag in soil has not been fully explored. For instance, oxidation from Ag^0 to Ag^+, or the release of Ag^+ from organic matter, has been shown to occur and is driven both chemically[14] and biochemically.[15]

Among the various species of Ag, ionic Ag^+ is considered the most effective antimicrobial form.[16] Known or suspected biocidal Ag mechanisms include: protein function inhibition caused by Ag binding to bisulfide bonds; interference with the electron transport chain; inhibition of DNA replication and transcription via macromolecule binding; and reactive oxygen species (ROS) mediated cell death.[17−20] Importantly, microbial cell debris can also act as a Ag reservoir, retaining the ability to exert biocidal activity on living microbial cells,[21] possibly via chemical and/or enzymatic Ag^+ release mechanisms.

Widespread concern regarding the environmental fate of engineered Ag nanoparticles (Ag-NP) has stimulated interest

Received: February 3, 2018
Revised: April 17, 2018
Accepted: June 27, 2018
Published: June 27, 2018

DOI: 10.1021/acs.est.8b00677
Environ. Sci. Technol. 2018, 52, 8745−8755

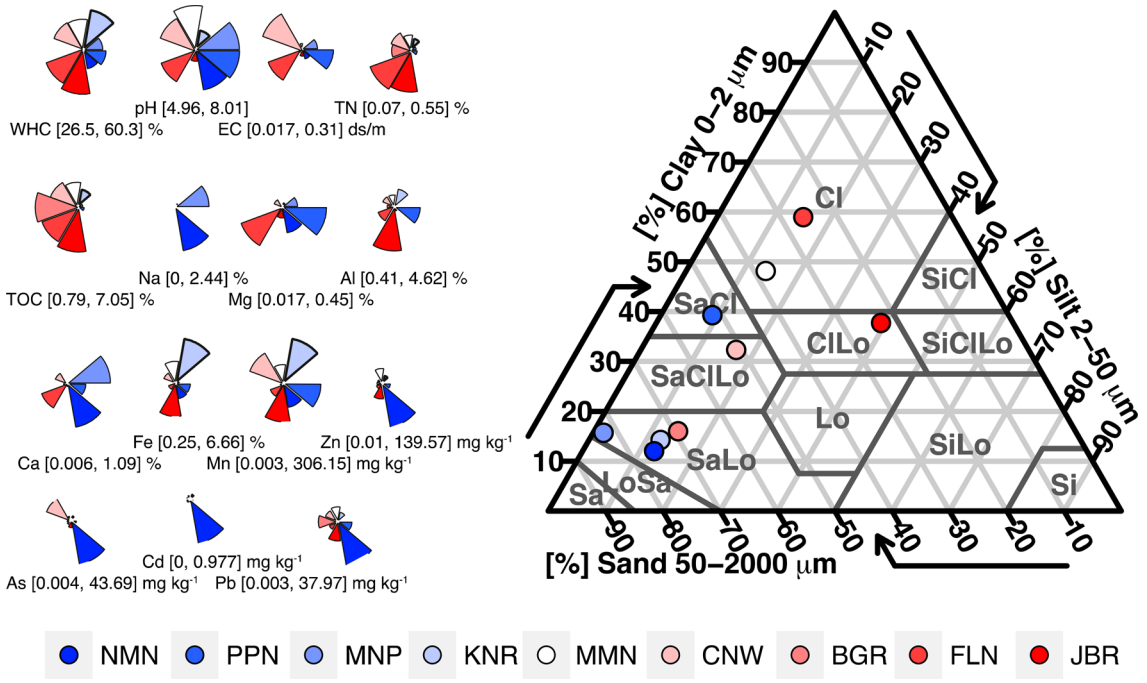

Figure 1. Chemical properties (left, star-plots) and texture (right, USDA triangle) of the soils used in this study. The color key provides a link between the soil textures and soil names as given in Table 2, while the soils are ordered according to TOC content in ascending order (left to right). The USDA soil texture classification triangle abbreviations resolve to sand (Sa); loamy sand (LoSa); sandy loam (SaLo); sandy clay loam (SaClLo); sandy clay (SaCl); clay (Cl); clay loam (ClLo); loam (Lo); silty clay (SiCl); silty clay loam (SiClLo); silty loam (SiLo); silt (Si).

regarding their possible toxicity to soil microorganisms.[22] Nevertheless, Ag toxicity in the environment (and especially the toxicity of ionic Ag) remains relatively understudied when compared with toxicity assessments of other metals,[23] and detailed research into the effects of Ag on soil microbial communities is warranted. Studies by Colman et al.[24] and Schlich et al.[25] investigated the effects of low level Ag^+ and Ag nanoparticle (Ag-NP)-fortified biosolids additions to soil (0.7–4 mg kg^{-1} of Ag in topsoil[24,25]). Colman et al.[24] found transient effects of Ag on soil microbial community structure and other microbial biomarkers (enzymatic activities and N_2O flux). Schlich et al.[25] found equal or enhanced inhibition of the soil microbial biomass and microbial functions in soils treated with Ag^+ compared with Ag-NP treated sludge. Both Ag^+ and Ag-NPs had a significant impact relative to the untreated sludge. While both of these studies provided valuable insights into the potential impacts of Ag on receiving ecosystems, they each focused only on a single soil type. In a previous study,[11] we reported on the changes in soil microbial communities and diversity in five soils treated with three dose rates of Ag (added as Ag^+) and observed that soil type is an important determining factor on Ag impact. However, to date, only Langdon et al.[23] have reported Ag EC_{50} values specifically in relation to a soil microbial process (nitrification). They found that EC_{50} values for nitrification varied greatly across the six soils included in their study, with values ranging from 0.43 to >640 mg Ag kg^{-1}. These findings highlight the potential variation in Ag toxicity between soils and indicate the need to develop a mechanistic understanding of the factors underpinning this variability. Moreover, while nitrification is recognized as a sensitive and important end point in relation to metal toxicity, there is currently no detailed information available with respect to Ag toxicity thresholds for other microbial biomarkers. Associated insights would serve to increase the predictive capacity of ecotoxicological models and also increase our understanding of the ecology of metal-affected ecosystems.

In the present study, we significantly expand the available information on Ag terrestrial ecotoxicology by assessing how Ag^+ (supplied as $AgNO_3$) affects an array of extracellular soil enzyme activities related to the C, N, P, and S cycles, substrate induced microbial respiration, and bacterial and fungal abundances. Ionic Ag (Ag^+) was investigated as its microbial toxicity is well established and because it is the common Ag species derived from the dissolution of Ag-containing NPs independently of their composition, size, shape, and surface functionalization. We also examined the relationship between soil properties (e.g., total organic carbon (TOC) and pH) and toxicity thresholds by using a set of nine diverse soils dosed at nine different Ag^+ levels.

MATERIALS AND METHODS

Soil Characterization. Samples of topsoils (0–20 cm) were collected from nine locations across Australia (Tables 2 and Table S1; Figure 1 and Figure S1), air-dried and sieved to <2 mm. Soils were collected from noncultivated areas to minimize the influence of agrochemicals. Soil texture analysis was performed using the method described by McKenzie et al.[26] and water holding capacity (WHC) determined as described previously.[27] The soil electrical conductivity (EC) and pH were measured after suspending the soil in water at a 1:10 ratio and shaking overnight at 150 rpm on an end-over-end shaker. Total organic carbon (TOC) and total nitrogen (TN) were analyzed with the combustion method using ca. 0.2 g of air-dried soil (acidified for TOC analysis) with a LECO CNS analyzer (LECO, Saint Joseph, MI). Multielemental analysis was performed after digestion of 200–250 mg of air-dried soil in 10 mL of reverse aqua regia (20% v/v of 37% HCl

DOI: 10.1021/acs.est.8b00677
Environ. Sci. Technol. 2018, 52, 8745–8755

Table 1. Information on the Analyzed Enzyme Activities and Associated Substrates

enzyme	enzyme consort. (EC) no.	code	dye−substrate conjugate	buffer pH	nutrient cycle
α-1,4-glucosidase	3.2.1.20	AG	4-methylumbelliferyl α-D-glucopyranoside	5.5	C
β-1,4-glucosidase	3.2.1.21	BG	4-methylumbelliferyl β-D-glucopyranoside	5.5	C
β-D-cellobiohydrolase	3.2.1.91	CB	4-methylumbelliferyl β-D-cellobioside	5.5	C
β-xylosidase	3.2.1.37	XYL	4-methylumbelliferyl-β-D-xylopyranoside	5.5	C
β-1,4-N-acetylglucosaminidase	3.2.1.96	NAG	4-methylumbelliferyl N-acetyl-β-D-glucosaminide	7.5	N
L-leucine aminopeptidase	3.4.11.1	LAP	L-leucine-7-amido-4-methylcoumarin hydrochloride	7.5	N
acid phosphatase	3.1.3.2	PHac	4-methylumbelliferyl phosphate	5.5	P
alkaline phosphatase	3.1.3.1	PHal	4-methylumbelliferyl phosphate	7.5	P
arylsulfatase	3.1.6.1	SUL	4-methylumbelliferyl sulfate potassium salt	5.5	S

Table 2. Soil Properties and Site Collection Details[a]

site name	state	pH	TOC (%)	clay (%)	silt (%)	sand (%)	Fe (%)	Al (%)
Newman (NMN)	WA	7.8	0.79	11.72	12.21	73.71	2.31	0.65
Pinpinio (PPN)	VIC	7.95	1.27	39.58	9.06	52.08	2.28	2.81
Minnipa (MNP)	SA	8.01	1.48	15.66	1.8	82.26	0.56	0.41
Kingaroy (KNR)	QLD	6.12	2.92	13.37	11.71	68.72	6.66	2.04
Myamyn (MMN)	VIC	6.84	3.05	42.24	12.19	33.32	2.14	1.03
Coonawarra (CNW)	SA	7.63	5.2	29.15	15.03	46.04	1.88	1.46
Barren Grounds (BGR)	NSW	4.96	5.49	16	14.67	69.33	0.25	0.74
Fox Lane (FLN)	SA	7.49	6.1	59.03	15.05	26.05	1.34	2.01
Jamberoo (JBR)	NSW	5.66	7.05	37.75	39.23	23.1	5.02	4.62

[a]Soils are ordered according to TOC content.

and 80% v/v of 70% HNO_3), using a microwave digestion system (MARS 6, CEM Corporation, Matthews, NC). The digests were filtered through 0.22 μm syringe filters and analyzed by inductively coupled plasma−mass spectrometry (ICP-MS; Agilent 8800 Santa Clara, CA). Analysis of a USA Department of Commerce standard soil reference material (SRM; 2711a Montana II soil) was used for digestion/ICP-MS method quality control. The recoveries were typically within 10% of the certified values. The Triple Quadrupole ICP-MS used in the study gives a Ag detection limit of 0.05 $\mu g\ l^{-1}$.

Microcosm Setup. For each air-dried soil, 135 g samples were weighed into bags and spiked with 10 mL of aqueous $AgNO_3$ using a hand sprayer. Final nominal total Ag concentrations were 0, 1, 25, 50, 100, 250, 500, 1000, and 2000 mg kg^{-1}. The soils were incubated at 25 °C overnight and subsequently leached with artificial rainwater until the EC of the leachate was similar to that of the control soil with no Ag added (this generally required leaching with 2−3 times the pore volume of the soil); this was done to minimize the confounding effects of excess salinity and to remove excess nitrate as described previously.[28] Artificial rainwater was used for this leaching process as described by Broos et al.,[29] with chloride salts deliberately avoided in order to prevent the formation of AgCl precipitates. The leached soils were then air-dried at 25 °C in the dark (to prevent Ag^+ photoreduction) for 2−3 weeks and split into three 40 g portions, each operationally defined as a replicate. Humidity was then set to 30% of the soil water holding capacity (WHC), and the soils were incubated for a further 2 months at 25 °C in the dark. The water content was corrected twice a week.

At the end of the incubation period, the microcosms were sampled and immediately analyzed for substrate induced microbial respiration. Subsamples were frozen at −20 °C for downstream screening of a range of extracellular enzyme activities and total DNA screening for microbial marker genes. Subsamples were also left to air-dry and were subsequently used to verify the total Ag soil content post spiking/leaching using the same acid digest/ICP MS method described previously for the multielemental soil characterization.

Soil Substrate Induced Microbial Respiration Activity. Substrate-induced respiration (SIR) activity was measured using the MicroResp system[30] as previously described by Wakelin et al.[31] Briefly, ca. 8 × 300 mg of each soil sample was uniformly loaded into 8 × 1.2 mL wells in 96-well microplates (i.e., one column in the microplate) taking care to avoid soil compression. The soil mass was recorded immediately after each column was filled, and the filled wells were covered with Parafilm M (BEMIS, Neenah, WI) to prevent water loss. Aliquots of D-(+)-glucose (equivalent to 7.5 mg g^{-1} of soil pore water) were added to the top of each well in 30 μL of aqueous solution. Indicator microplates with 3% agarose gel containing 12.5 $\mu g\ mL^{-1}$ Cresol red, 150 mM KCl, and 2.5 mM $NaHCO_3$ were colorimetrically analyzed before the assay (570 nm absorbance using the Synergy HT microplate absorbance/fluorescence reader; Bio-Tek, Winooski, VT) and were then secured with a rubber seal to the microplate assembly containing the soil samples and glucose substrate. The plates were incubated at 25 °C for 6 h after which the CO_2-induced color changes of the Cresol red indicator plates were recorded and the CO_2 production rates were calculated as per the MicroResp manufacturer's instructions.

Enzyme Activities. Nine soil enzyme activities were analyzed using fluorescently labeled substrates as previously described by Bell et al.[32] The fluorescent dyes, which are quenched by the substrate when conjugated, were 4-methylumbelliferone (MUB) and 7-amino-4-methylcoumarin (AMC). Further relevant details pertaining to the measured enzymatic activities are provided in Table 1.

Each soil sample was blended in a buffer solution to dissolve the enzymes, and the resulting soil slurry was incubated together with the fluorescently labeled substrate. When performing enzyme assays, the choice of buffer pH can either

DOI: 10.1021/acs.est.8b00677
Environ. Sci. Technol. 2018, 52, 8745−8755

be matched to the actual soil pH or to the optimal pH for each specific enzyme activity.[33] For the present study, we tested enzyme activities at two different pH values: pH 5.5 established using 50 mM sodium acetate buffer, and pH 7.5 established using 50 mM Tris buffer, approximating the optimal pH for the different enzymatic tests (Table 2), as suggested by Niemi and Vepsäläinen.[33] For each soil sample, 2.75 g of soil was mixed in a blender with 91 mL of buffer. The resulting slurry was transferred into a container with continuous stirring and used to measure all enzyme activities for that soil sample. Standard curves for the MUB and AMC based dyes were set up in two control plates for each soil slurry. For each test, 800 μL of slurry was incubated with either 200 μL of 0.2 mM of fluorescently labeled substrates in the test plate or 200 μL of 0, 2.5, 5, 10, 25, 50, and 100 μM dye solutions (MUB or AMC) in the corresponding control plates (for establishing standard curves and controlling for background soil fluorescence/quenching). The test and control plates were incubated at 25 °C in the dark for 3 h. Post incubation, the plates were centrifuged for 3 min at 2900*g*, and 250 μL of each supernatant was transferred into black plates and analyzed with the FLUOstar Optima (BMG Labtech, Cary, NC) microplate absorbance/fluorescence reader using the 355/460 nm excitation/emission filter-set. The substrate degradation rates were calculated according to the control plate standard curve intensity values.

Soil DNA Extraction and Quantification of Total Bacterial and Fungal Genetic Markers. Soil DNA was extracted using the FastDNA Spin kit for Soil and a FastPrep bead beating instrument (MP Biomedicals, Santa Ana, CA) according to the manufacturer's instructions. The bead beating step was performed three times for 60 s at 6.5 m/s. DNA extracts were quantified with the Quant-iT HS ds-DNA assay kit in a Qubit fluorometer (Invitrogen, Carlbad, CA) according to the manufacturer's instructions. DNA extracts diluted to 0.1 ng μL^{-1} were used as templates in the polymerase chain reaction (PCR) based screening of the markers as described below. Total bacterial 16S rRNA gene counts were analyzed with real-time quantitative PCR (qPCR) on a CFX Connect (BioRad, Hercules, CA) instrument in 20 μL volumes comprising 2 μL of template DNA, 0.4 μL of 20 mg mL^{-1} PCR grade bovine serum albumin (BSA) for reducing potential PCR inhibition due to impurities;[34] 5.6 μL of PCR grade H_2O; 10 μL of the 2 X Kapa SYBR fast master-mix (Kapa Biosystems, Wilmington, MA); 1 μL of the 10 μM forward primer (5′-TCCTACGGGAGGCAGCAGT-3′) and 1 μL of the 10 μM reverse primer (5′-GGACTACCAGGGTATCTAATCCTGTT-3′) developed by Nadkarni et al.[35] A two-step reaction was performed according to the Kapa SYBR fast manufacturer instructions using 3 min at 95 °C for initial enzyme hot-start activation, then 40 cycles of 3 s at 95 °C for denaturation, and 30 s at 60 °C for primer annealing and elongation. The size of the fungal community was similarly assessed, using qPCR targeting the intergenic spacer (ITS) region. The same protocol as that of the bacterial primers was followed, but the forward and reverse primers were 5′-TCCGTAGGTGAACCTGCGG-3′ and 5′-CGCTGCGTTCTTCATCG-3′, respectively, as described by Fierer et al.[36]

Absolute quantification was performed using single insert standards generated by PCR with the 27F (AGAGTTTGATCCTGGCTCAG) and 1492R (GRTACCTTGTTACGACTT) primers[37] on *Escherichia coli* JM109 (ATCC 53323) genomic DNA extracts for the total bacterial 16S rRNA gene counts and using standards generated via cloning in the case of the fungal ITS.[11] Primer efficiencies were 97% for the bacterial 16S rRNA gene fragment and 91% for the fungal ITS, and multiple no template controls were included for quality control.

Statistical Data Analysis. Biomarker dose−response modeling was performed using normalized data, whereby biomarker values were divided by the mean value of the matching unamended control soil (i.e., the Ag 0 mg kg^{-1} treatment). Analyses were carried out using the dose response curves (drc) v2.5−12 package[38] in R,[39] and a brief description of the tested models can be found in Ritz et al.[40] An empirical modeling approach was used by selecting the best fitting model. Goodness of fit (GoF) indices used in the model selection were: Akaike information criterion (AIC) values (used as the major criterion for model selection); standard deviation of the residuals; standard error of the EC_{50} values; weighted coefficient of determination (R^2) as implemented in the qpcR v1.4−0 package[41] (based on the models' lack of linearity as opposed to the standard coefficient of determination[42]); and the lack of fit approach. Pearson product moment correlation tests were also performed between the log transformed (i.e., normally distributed) activity/marker-count values and between the resulting EC_{50} values and soil properties data.

RESULTS

Soil Properties. The topsoils (0−20 cm) used in this study were sampled across a wide geographic area, representing a broad variety of soil types and physicochemical characteristics (Table 1 and Table S1, Figure 1 and Figure S1).

The texture of the collected soils (Figure 1) included sandy loam (KNR, BGR, NMN, MNP), sandy-clay (PPN), sandy-clay-loam (CNW), clay-loam (JBR), and clay (MMN, FLN). Organic carbon ranged from 0.8 to 7%, and the soil pH ranged from acidic (pH 5.0) to alkaline (pH 8.0). Principal components analysis (PCA) using the z-scores of these parameters along with WHC, EC, TN, Na, Mg, Al, Ca, Fe, Mn, Zn, As, Cd, and Pb as inputs, was performed to obtain an overview of the variability in soil properties across the soils used in our study (Figure S1). This analysis revealed large differences between the soils, with NMN being the most disparate.

Dose−Response Model Fitting. The effects of increasing Ag doses were assessed for a range of different biomarkers, including SIR, 16S rRNA, and ITS counts, and nine different soil enzyme activities. As modeling via a single parsimonious formula was not possible for several of the measured biological parameters, we used an empirical approach and selected the AIC best scoring models for each biomarker and soil type. The main reason for this was that hormesis-like responses were found more frequently in some soils (Table S2 and Figure S2). A good example of this is seen in the FLN soil, where the activities of LAP, PHal, SUL, AG, BG, CB, PHac, and XYL all provided hormesis-like responses whereas the other soil biological parameters fitted log−logistic family models. Three more soils (MNP, JBR, and BGR) also showed hormesis-like responses in 4 out of 12 measured biological variables. Although the incidence of hormesis-like responses seems somewhat soil-specific, activity-specific discrimination was also demonstrated since NAG and LAP had more hormesis-type responses (found in five out of nine soils) compared with other measured biomarkers. The goodness of fit statistics showed

DOI: 10.1021/acs.est.8b00677
Environ. Sci. Technol. 2018, 52, 8745−8755

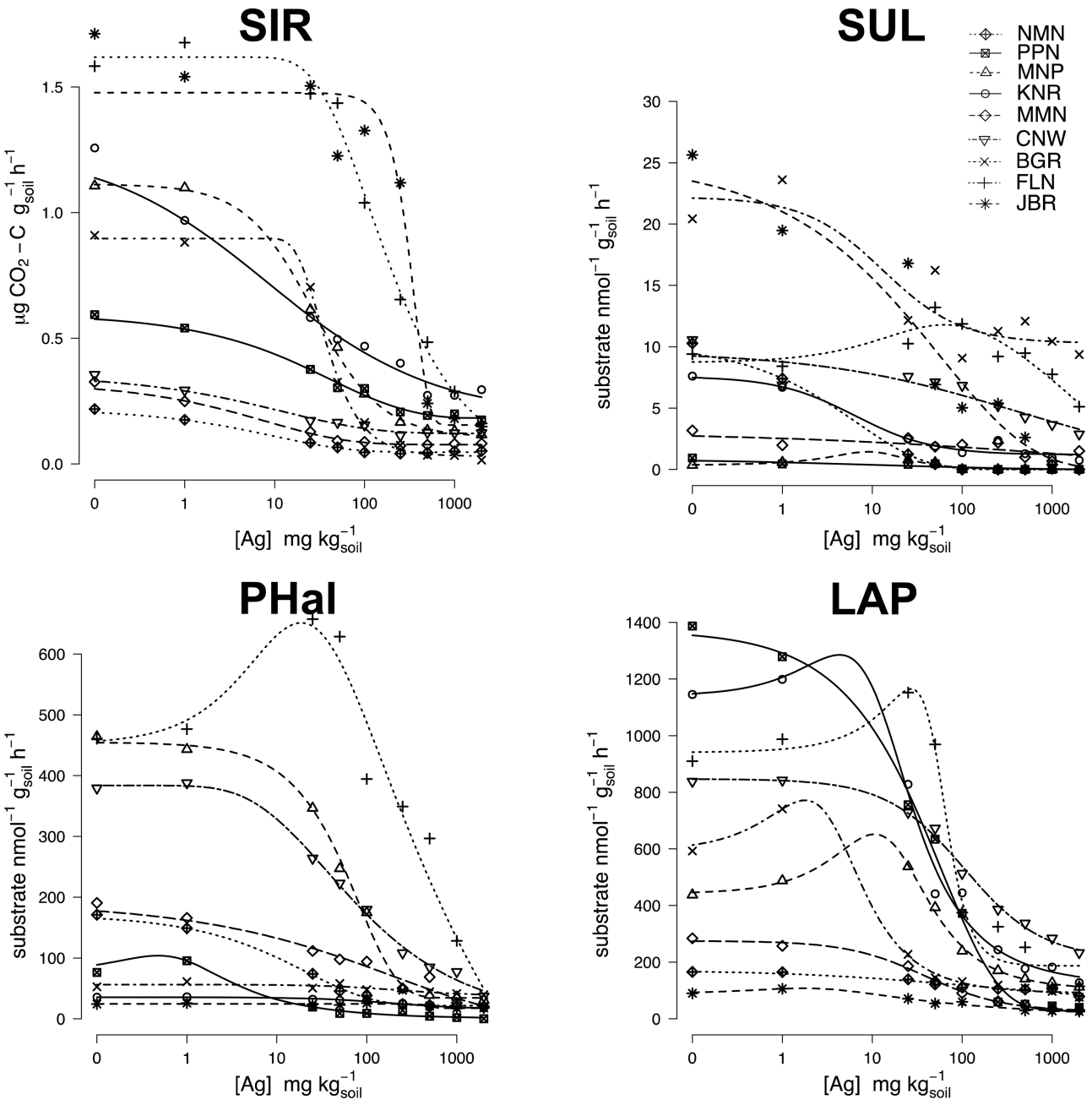

Figure 2. Dose−response model fitting for substrate induced respiration (SIR), sulfatase (SUL), alkaline phosphatase (PHal), and L-leucine aminopeptidase (LAP) in the nine different soils (the complete range of tested biomarkers for all soils is presented in Figure S2). Each point comprises the mean value of three biological replicates. Models showing the AIC-based best fits included a range of log−logistic and nonmonotonous hormesis models.

that some biological parameters varied less than others and were better described by the models. SIR for example, had the highest weighted R^2 value among measured parameters with an average of 0.98. LAP, PHal, NAG, and 16S rRNA gene copies followed with weighted R^2 of >0.88, while the rest of the parameters had lower weighted R^2 values (down to 0.63 for ITS and SUL.

EC_{50} Values. EC_{50} values for SIR in the different soils varied by 2 orders of magnitude, from 3.3 to 434.7 mg Ag kg^{-1} (Figure 2). The complete data and fitted curves are shown in Figure S2, and the EC50s, standard errors, and R^2 for all the biomarker−soil combinations are reported in Table 3. Among the biomarkers investigated, SUL and LAP were the most sensitive with mean EC_{50} values across all soils of 21.8 and 37.6 mg Ag kg^{-1}. These were followed by PHac, XYL, AG, and SIR (52.1−69.3 mg Ag kg^{-1}), while the remaining parameters showed lower sensitivity to added Ag^+. The bacterial 16S rRNA gene abundance was more sensitive to Ag^+ addition than the fungal ITS abundance (EC50s of 89.3 and 202 mg kg^{-1}, respectively). On average the PPN, FLN, and MMN soils (with 1.3%, 6.1% and 3.0% TOC, and pH 7.9, 7.5 and 6.8, respectively) had the lowest EC_{50} values across the biological parameters examined (35.8−47.7 mg kg^{-1}), whereas CNW and KNR had the highest average EC50 values (163 and 196.3 mg kg^{-1} respectively; with TOC values of 5.2% and 2.9% and pH values of 7.6 and 6.1 for these two soils).

DOI: 10.1021/acs.est.8b00677
Environ. Sci. Technol. 2018, 52, 8745−8755

Table 3. Model-Predicted Biomarker EC_{50} Values for Each soil (mg Ag kg^{-1})[a,b]

soil	statistic	SUL	LAP	PHac	XYL	AG	SIR	16S	PHal	NAG	CB	BG	ITS	mean
NMN	EC_{50}		50	44.2	6.8	1.7	9.1	3.1	21.5	8.2	2.6	90	605.5	**76.6**
	st err (% of EC_{50})		67.40%	7.20%	18.00%	18.60%	9.80%	36.00%	12.10%	30.90%	13.20%	13.20%	33.00%	**24.60%**
	R^2		0.84	0.98	0.98	0.93	0.99	0.94	0.99	0.98	0.82	0.94	0.51	**0.9**
PPN	EC_{50}	9.8	59.5	147.5	12.5	6.1	5.1	9.4	0.6	7.9	5.7	120.1	44.9	**35.8**
	st err (% of EC_{50})	265.60%	6.80%	22.60%	12.80%	31.70%	21.50%	46.20%	127.60%	40.60%	23.70%	10.70%	33.00%	**53.60%**
	R^2	0.45	0.99	0.87	0.98	0.96	0.97	0.9	0.97	0.93	0.98	0.97	0.87	**0.9**
MNP	EC_{50}	11.3	16.5	158.5	86	118.5	3.3	439.3	82.2	58.5	134.8	5.3	256.7	**114.3**
	st err (% of EC_{50})	48.60%	31.00%	9.30%	11.30%	10.80%	1.50%	93.60%	4.10%	22.30%	11.80%	1.90%	22.70%	**22.40%**
	R^2	0.66	0.99	0.97	0.96	0.96	0.99	0.81	1	0.95	0.95	0.95	0.82	**0.92**
KNR	EC_{50}	6.3	11.8	2	45.7	2	8.2	9.9	5.3	1.2	479	467.8	266.1	**108.8**
	st err (% of EC_{50})	33.30%	34.40%	68.60%	83.00%	113.70%	47.50%	46.30%	9.10%	114.60%	8.70%	29.60%	29.70%	**51.50%**
	R^2	0.92	0.98	0.91	0.62	0.78	0.93	0.9	0.85	0.97	0.61	0.59	0.78	**0.82**
MMN	EC_{50}	14.3	38.9	15.3	1.8	0.4	8.2	23	202	0.3		193.8	4.5	**45.7**
	st err (% of EC_{50})	110.80%	12.40%	72.50%	94.70%	187.50%	13.70%	15.60%	114.50%	365.70%		47.50%	16.40%	**95.60%**
	R^2	0.53	0.98	0.31	0.51	0.21	0.99	0.86	0.96	0.94		0.5	0.32	**0.65**
CNW	EC_{50}	13.2	101.2	1.6	150.5	225.4	23.6	252.8	36.2	959.6	29.7	12.8	149.8	**163**
	st err (% of EC_{50})	209.10%	16.70%	50.20%	25.00%	47.10%	15.30%	120.40%	9.10%	50.10%	37.20%	85.10%	24.20%	**57.50%**
	R^2	0.45	0.96	0.92	0.79	0.48	0.98	0.88	0.99	0.69	0.91	0.92	0.76	**0.81**
BGR	EC_{50}	13.1	3.4	75.6	191.2	71.6	20.2	2	225	14.8		205.3	46.5	**78.9**
	st err (% of EC_{50})	65.10%	121.50%	24.00%	21.80%	28.90%	6.50%	24.90%	58.10%	27.40%		43.60%	20.90%	**40.20%**
	R^2	0.68	0.97	0.57	0.85	0.62	0.99	0.93	0.73	0.93		0.84	0.58	**0.79**
FLN	EC_{50}	49.2	54.4	2.9	5	46	111.7	60.3	21.8		9.6	51.4	8.4	**38.2**
	st err (% of EC_{50})	99.40%	12.30%	29.30%	28.50%	39.70%	6.90%	31.00%	43.40%		94.40%	38.90%	250.00%	**61.20%**
	R^2	0.52	0.96	0.8	0.92	0.9	0.99	0.77	0.94		0.78	0.8	0.28	**0.79**
JBR	EC_{50}	56.9	2.3	21.3	6.4	62.7	434.7	4	512.2	7.3	357.6	454.7	436.1	**196.4**
	st err (% of EC_{50})	44.50%	43.80%	22.20%	41.40%	36.60%	16.10%	4.30%	7.40%	8.50%	26.70%	35.70%	31.70%	**26.60%**
	R^2	0.8	0.95	0.93	0.86	0.81	0.97	0.95	0.81	0.99	0.77	0.73	0.79	**0.86**
mean	**EC_{50}**	**21.8**	**37.6**	**52.1**	**56.2**	**59.4**	**69.3**	**89.3**	**123**	**132.2**	**145.6**	**177.9**	**202**	
	st err (% of EC_{50})	**109.50%**	**38.50%**	**34.00%**	**37.40%**	**57.20%**	**15.40%**	**46.50%**	**42.80%**	**82.50%**	**33.70%**	**34.00%**	**51.30%**	
	R^2	**0.63**	**0.96**	**0.81**	**0.83**	**0.74**	**0.98**	**0.88**	**0.92**	**0.92**	**0.83**	**0.8**	**0.63**	

[a]Standard errors expressed as percentages of the EC_{50} values and the model locally weighted R^2 values are also given. Empty cells imply no model fit. Soils are ordered according to increasing TOC content (top to bottom), while the biomarkers are ordered according to increasing sensitivity (left to right). [b]16S = bacterial 16S rRNA gene quantities, ITS = fungal SSU gene quantities and SIR = substrate induced respiration (MicroResp). The following reference enzyme activities: NAG = acetylglucoaminase; LAP = leucine aminopeptidase; Phal = alkaline phosphatase; SUL = arylsulfatase; AG= glucosidease; BG = glucopyranoside; CB = cellobioside; PHac = acid phosphatase; XYL = xylopyranoside; st err: the EC50 standard errors expressed as % of the predicted EC50; R^2: the weighted coefficient of determination of the model fit.

Environ. Sci. Technol. 2018, 52, 8745−8755 DOI: 10.1021/acs.est.8b00677

Correlations between Measured Biological Parameters. Pearson correlations between the $\log_{10}$ transformed biomarker values are summarized in Figure 3 (full correspondanalysis based on the correlations of the log-transformed values showed strong associations among the carbon cycle-related AG, BG, CB, and XYL biomarkers (with PHac also grouping closely with SIR and the total bacterial 16S rRNA gene counts). The sulfur, nitrogen, and phosphorus activities showed a more scattered pattern.

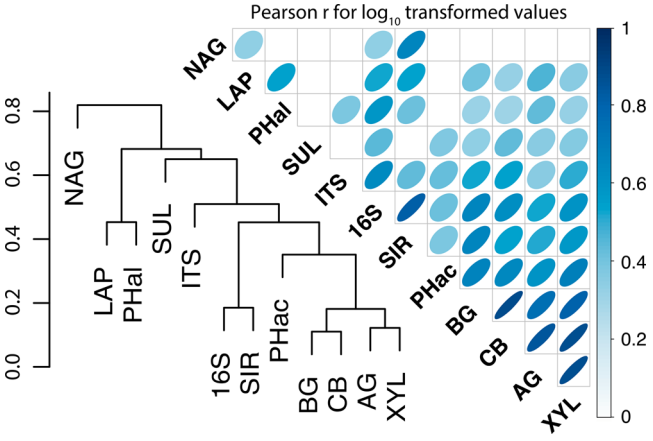

Figure 3. Correlation analysis results for the analyzed biological parameters. The upper right panel provides the Pearson correlation test results for the tested pairs using their log transformed values (ellipse forms and colors indicate the significant correlation coefficient value trends: blue/sharp indicate strong positive; round/white or missing indicate no significant correlation), while their correlation coefficient-based hierarchical clustering (UPGMA) (using $1 - r$ as a dissimilarity measure) is presented in tree form in the lower-left panel. No significant negative correlations were identified on the basis of this analysis. Significant correlation coefficients were determined using the Bonferroni approach for P value adjustment for multiple hypothesis testing ($\alpha \leq 0.01$).

ing regressions are provided in Figure S3), and are presented together with a dendrogram depicting their hierarchical clustering on the basis of these correlation coefficients. Overall, the bacterial 16S rRNA gene counts were more strongly and consistently correlated with the tested biomarkers than were the fungal ITS values. SIR was positively correlated with all tested biomarkers except for SUL, and a strong correlation was observed between SIR and 16S rRNA gene copies. Among the enzymatic activities, NAG was the least commonly correlated to the other parameters tested (3/11 correlations observed), whereas BG, CB, AG, and XYL were correlated with all other biomarkers tested, with the exclusion of NAG. Clustering

Correlation between Estimated End Points and Soil Characteristics. Correlation tests were performed to assess the importance of soil characteristics on the EC_{50} values of the biomarkers. TOC and pH were found to be relatively good predictors of the EC_{50} responses according to correlation tests (Figure 4), regression analysis (Figure S4), and principal component analysis that placed them in two separate soil property groups (Figure S1 middle-right panel). TOC had significant positive correlations with the EC_{50} values of SIR and SUL (thus suggesting less adverse Ag-effects on SUL and SIR in soils with greater TOC contents), and to a lesser degree with Phal and AG. Soil pH was positively correlated with LAP and 16S rRNA gene copy EC_{50} values and negatively correlated with BG, CB, and PHal EC_{50} values.

DISCUSSION

This study investigated the effect of Ag ions on 12 biomarkers in nine soils that varied across a range of edaphic factors. As such, this experimental design allows an investigation of (a) the correlations between different biomarkers to identify whether a representative subset of biomarkers can be selected for Ag risk assessment; (b) whether hormesis-like responses are soil- or biomarker- specific; and (c) if any particular soil variable is key to determining the response of the tested biomarkers. The discussion is articulated along this line.

Correlation Tests between Biomarkers. Silver, being a nonessential element with strong antibacterial properties,[16] had adverse effects on all biomarkers tested. Interestingly, Ag-induced effects also revealed underlying associations between the different biomarkers. For example, activities related to organic C mineralization were tightly correlated (Figure 3). XYL and CB have been recognized to act on more recalcitrant organic matter, while AG and BG are responsible for the degradation of the smaller oligo- and disaccharides into monosaccharides.[43−45] This cluster of enzyme activities was also correlated with SIR and the bacterial abundance marker (16S rRNA gene), which is consistent with these enzymatic

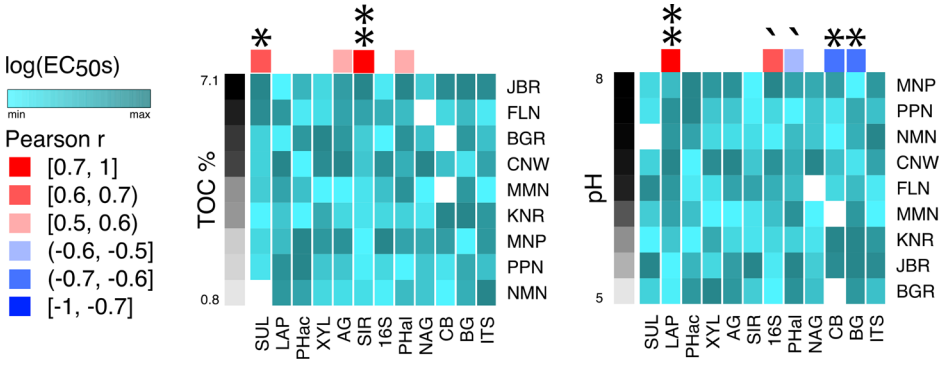

Figure 4. Heatmaps showing the correlations of soil TOC (%) and pH with the per-soil log transformed EC_{50} estimates of the measured biological parameters. The soils are ordered in descending order of TOC or pH (see gray scale on left). The different blue-range colors depict the EC_{50} value intensity, and correlations ($|r| \geq 0.5$) between the log transformed EC_{50}'s and the physical-chemical parameter of interest are denoted at the top of the heatmaps using the green/red colors provided in the key and with the statistical significance shown using the symbols ** for 0.01, * for 0.05, ′ for 0.1).

DOI: 10.1021/acs.est.8b00677
Environ. Sci. Technol. 2018, 52, 8745−8755

activities being ubiquitous among the bacterial heterotrophic community members that are dominant in nearly all soils.

The nitrogen cycle-associated activities of NAG (chitin degradation) and LAP (amino acid cleavage from N-terminus with preference to leucine)[46−48] were not associated in the cluster analysis, suggesting little linkage between these nutritionally disparate activities.

Sulfatase (SUL) was the most sensitive to Ag^+ addition of all the investigated enzymatic activities. SUL activity had a different response compared with the other enzymatic activities, the fungal and bacterial counts, alkaline phosphatase activity, and SIR (Figure 2 and Figure S2). In this context, it is important to note that Ag is known to have high affinity for molecules containing reduced sulfur, which could possibly render them as Ag reservoirs.[49] Our results thus raise questions about the effects of Ag on parameters that may affect the sulfatase activity at multiple levels. For instance, Ag could directly affect SUL functionality, select for microorganisms with differential sulfatase production capacity, or cause a decrease in the availability of reduced sulfur species, thus inducing sulfur deficiency. Sulfur starvation conditions are known to induce sulfatase production in bacteria.[50,51] Enhanced sulfatase production may be energetically costly for the extracellular enzyme producers, potentially reducing their survival capacity.

These results suggest that future research may not require the investigation of multiple C-cycle enzymes in addition to SIR, as their responses are collinear. It is also suggested that SUL, given its high sensitivity and lack of correlation with other biomarkers, should be closely monitored when investigating Ag toxicity in soil.

Hormesis-Like Responses of Microbial Biomarkers to Ag. In several cases, the dose−response curves fitted a hormesis-type response (e.g., see Figure 2 and Figure S2). Among the biomarkers and soil types, NAG and LAP and the FLN soil had the highest incidence of hormesis responses. This effect is freely translated in toxicology as the nonmonotonic response of a biological agent/system to a physical/chemical/biomolecular factor, where a reversal in response is observed between low and high doses.[52,53] It has been attributed to stimulatory or adaptive mechanisms, but remains poorly understood,[52] and its interpretation becomes even more difficult in highly complex and diverse biological systems like soil. Previous studies yielded hormesis-like responses in soil activities under Ag stress,[23,25,54,55] and it was proposed that increased metabolism at low effective metal doses could be associated with homeostatic responses overcompensating for the stress energy costs.[55] Support for this hypothesis has also been previously provided, where increased activity of leucine aminopeptidase was associated with oxidative stress in both higher organisms and bacterial strains.[46,47,56]

In the present study, hormetic-like patterns were often observed at the level of microbial activities (enzymatic and SIR), and also in some cases for microbial phylogenetic marker gene counts (Figure S2). This suggests that differential effects of Ag on microbial community members may allow more Ag-tolerant/resistant, but otherwise less competitive, microbial groups to become more competitive and active at low Ag concentrations. We have previously reported such a shift in soil microbial community structure where short-term Ag exposure tended to select for copiotrophs, whereas long-term exposure selected for k-strategists (oligotrophs, slow growers).[11]

Biomarker Ag Sensitivity and EC_{50} Correlations with Soil Properties. A large variation in EC_{50} values was observed across the different soils and biomarkers examined (Table 2, Figure S2). Sulfatase inhibition was the most consistent ecotoxicological end point tested with EC_{50} values ranging less than 10-fold (from approximately 6 to 57 mg kg^{-1}) while NAG showed the largest variability in EC_{50} between soils. This difference in effect size across soil types is not uncommon when metal toxicity and different microbial end points are considered. For instance, Smolders et al.[57] reported the toxicity threshold for Cu and Ni in 19 soils and found that toxicity values varied between 19- and 90-fold across the different soils, depending on the particular metal and assay considered (nitrification, glucose induced respiration, and maize residue mineralization). Overall, in our study, estimated EC_{50} values indicate significant effects on the SIR activity carried out by the heterotrophic microbial community at Ag concentrations between 3.3 and 9.1 mg kg^{-1} in five out of the nine tested soils. Moreover, there were a number of cases where Ag EC_{50} concentrations were below 1 mg kg^{-1} (with robust model fits), demonstrating that Ag may have adverse effects at environmentally relevant concentrations (recent meta-analysis[58] of Ag contents in soil reported concentrations from 0.1 to 51 mg kg^{-1}).

Across all biomarkers, the responses observed in our study were clearly soil-dependent. Our toxicity results support the findings of Langdon et al.[23] in terms of the range of observed Ag EC_{50} values and large variability between soils (EC_{50} values from 0.43 to >640 mg kg^{-1} soil were reported by Langdon et al.[23] for potential nitrification in six soils). Soil TOC and pH were found to be correlated with the EC_{50} values for some biomarkers (Figure 4). TOC positively correlated with the EC_{50}s for SIR (P = 0.0016) and SUL (P = 0.027) while, statistically nonsignificant, lower correlations were observed for PHal (P = 0.131) and AG (P = 0.137), thus showing lower overall Ag effects on heterotrophic and sulfate turnover activities at high TOC soil contents (Figure S4). This outcome is consistent with the well-documented Ag affinity for thiol groups in organic matter and its rapid conversion to nonreactive forms (e.g., Ag cysteine). For instance, Settimio et al.[8] found that over a 6-month period, lability (i.e., isotopic exchangeability) of Ag added to soil in ionic form decreased significantly, with a large proportion of Ag bound to reduced S species and a strong correlation of this Ag fraction with TOC.

The relationship between EC_{50} values and pH was less consistent. Soil pH is an important parameter affecting Ag chemistry and its soil-aging process,[8,59] but the relationship is not as simple as it is for many other metals (where pH is usually negatively correlated with metal bioavailability and toxicity). LAP EC_{50}s had a strong positive correlation with pH (P = 0.004), following a typical metal-pH pattern, where an increase in pH leads to a decrease in toxicity (i.e., higher pH leads to higher EC_{50} values). In contrast, EC_{50} values for BG and CB were negatively correlated with pH. This finding, and other observed variations in the correlations between pH and Ag toxicity in these soils, may be due to both chemical and biochemical factors. First, Ag speciation in soil is extremely complex with a variety of different Ag species being formed under different soil conditions. For instance, Sekine et al.[60] showed that the lability of Ag in soil (measured by diffusive gradient in thin films; DGT) was greater in soil under neutral and alkaline conditions than in the same soil at low pH (correlation P values of 0.037 and 0.048, respectively). This

DOI: 10.1021/acs.est.8b00677
Environ. Sci. Technol. 2018, 52, 8745−8755

was explained by X-ray absorption spectroscopy that showed the formation of Ag_2CO_3 at higher pH, as opposed to the transformation of Ag^+ to AgCl under acidic conditions; together this leads to comparatively greater Ag solubility at high pH. Furthermore, the pH optima for CB and BG activities reach maxima at pH values between 4 and 5.[33] Even though it was not statistically significantly correlated with either TOC or pH, PHal EC_{50}s does tend to increase with increasing TOC and decrease with increasing pH. Previously, Frankenberger and Johanson[61] showed that alkaline phosphatase (Phal) is active even at soil pH values as low as 4. Even though EC_{50} values should be independent of the pH optimum for each enzyme (unlike the absolute activity level of each enzyme in the soils of different pHs), we cannot assume that the sensitivity of the various enzymatic processes is completely decoupled from soil pH.

Implications for Risk Assessments of Ag in Soil. The Ag EC_{50}'s obtained in this study confirm the strong antimicrobial potential of this element and show that deleterious biological effects can occur at relatively low and environmentally relevant soil concentrations. Although these Ag concentrations are higher than the predicted concentrations of Ag in appropriately regulated biosolids amended soils (e.g., Sun et al.[7]), it should be kept in mind that, at this stage, predicted concentrations have not yet been verified experimentally and uncertainties remain regarding future trends in Ag usage. Given the fact that Ag behavior in soil is extremely complex, a broad range of biomarker testing is necessary to gain thorough insight into the predicted effects. To this end, studies like the one presented here, which report an extended data set of ecotoxicological responses to Ag in soil, may still need to be complemented by additional investigations. For instance, the negative correlations of some biomarkers (BG, CB) with soil pH should be further investigated and better understood, especially considering that in the case of Ag nanomaterials, the relationship between pH (and TOC) and toxicity may be even more complex than it is for ionic silver. For instance, Schlich and Hund-Rinke[62] reported that the toxicity of Ag nanoparticles increased with decreasing pH; this is most likely due to increased dissolution of metallic Ag.

This study also suggests that bacterial end points may be more appropriate and more sensitive than fungal assays and that, as enzymes involved in the C cycle are well correlated to each other, the effect of Ag in terms of this vital microbial function may be predicted by investigating one, rather than multiple, C-related end points. Finally, this study shows a strong, and often soil-specific, hormesis-like effect for Ag. While this is interesting from a mechanistic point of view, it should also be considered when assessing the long-term effect of Ag across a wider range of potential Ag concentrations.

■ ASSOCIATED CONTENT

Supporting Information

TThe Supporting Information is available free of charge on the ACS Publications website at DOI: 10.1021/acs.est.8b00677.

Figure captions for the supporting figures and two supporting tables (PDF)

Supporting figure 1 (PDF)

Supporting figure 2 (PDF)

Supporting figure 3 (PDF)

Supporting figure 4 (PDF)

■ AUTHOR INFORMATION

Corresponding Author

*E-mail: erica.donner@unisa.edu.au.

ORCID

Sotirios Vasileiadis: 0000-0002-2048-8192

Notes

The authors declare no competing financial interest.

■ ACKNOWLEDGMENTS

This project was supported by the Australian Research Council (FT100100337 and FT130101003).

■ ABBREVIATIONS

16S	16S rRNA gene copies
ITS	intergenic spacer copies
SIR	substrate induced respiration
NAG	β-1,4-*N*-acetylglucosaminidase
LAP	L-leucine aminopeptidase
PHac/al	acid/alkaline phosphatase
A/BG	α/β-1,4-glucosidase
CB	β-D-cellobiohydrolase
XYL	β-xylosidase
SUL	arylsulfatase.

■ REFERENCES

(1) Benn, T.; Cavanagh, B.; Hristovski, K.; Posner, J. D.; Westerhoff, P. The release of nanosilver from consumer products used in the home. *J. Environ. Qual.* **2010**, *39* (6), 1875−1882.

(2) Holtz, R. D.; Lima, B. A.; Souza Filho, A. G.; Brocchi, M.; Alves, O. L. Nanostructured silver vanadate as a promising antibacterial additive to water-based paints. *Nanomedicine* **2012**, *8* (6), 935−940.

(3) Lorenz, C.; Windler, L.; von Goetz, N.; Lehmann, R. P.; Schuppler, M.; Hungerbuhler, K.; Heuberger, M.; Nowack, B. Characterization of silver release from commercially available functional (nano)textiles. *Chemosphere* **2012**, *89* (7), 817−24.

(4) The DTU Environment, the Danish Ecological Council, and the Danish Consumer Council. *The Nanodatabase*, http://nanodb.dk/ (accessed 15/01/2018).

(5) Woodrow Wilson Institute Woodrow Wilson International Center for Scholars, Pew Charitable Trusts. *Project on Emerging Nanotechnologies*. 2005/rev. 2013 https://www.wilsoncenter.org/ (accessed 15/01/2018).

(6) Gottschalk, F.; Nowack, B. The release of engineered nanomaterials to the environment. *J. Environ. Monit.* **2011**, *13* (5), 1145−55.

(7) Sun, T. Y.; Conroy, G.; Donner, E.; Hungerbuhler, K.; Lombi, E.; Nowack, B. Probabilistic modelling of engineered nanomaterial emissions to the environment: a spatio-temporal approach. *Environ. Sci.: Nano* **2015**, *2* (4), 340−351.

(8) Settimio, L.; McLaughlin, M. J.; Kirby, J. K.; Langdon, K. A.; Lombi, E.; Donner, E.; Scheckel, K. G. Fate and lability of silver in soils: Effect of ageing. *Environ. Pollut.* **2014**, *191*, 151−157.

(9) Lombi, E.; Donner, E.; Taheri, S.; Tavakkoli, E.; Jämting, Å. K.; McClure, S.; Naidu, R.; Miller, B. W.; Scheckel, K. G.; Vasilev, K. Transformation of four silver/silver chloride nanoparticles during anaerobic treatment of wastewater and post-processing of sewage sludge. *Environ. Pollut.* **2013**, *176* (0), 193−197.

(10) Brunetti, G.; Donner, E.; Laera, G.; Sekine, R.; Scheckel, K. G.; Khaksar, M.; Vasilev, K.; De Mastro, G.; Lombi, E. Fate of zinc and silver engineered nanoparticles in sewerage networks. *Water Res.* **2015**, *77*, 72−84.

(11) Vasileiadis, S.; Puglisi, E.; Trevisan, M.; Scheckel, K. G.; Langdon, K. A.; McLaughlin, M. J.; Lombi, E.; Donner, E. Changes in soil bacterial communities and diversity in response to long-term silver exposure. *FEMS Microbiol Ecol* **2015**, *91* (10), fiv114.

DOI: 10.1021/acs.est.8b00677
Environ. Sci. Technol. 2018, 52, 8745−8755

(12) Kaegi, R.; Voegelin, A.; Sinnet, B.; Zuleeg, S.; Hagendorfer, H.; Burkhardt, M.; Siegrist, H. Behavior of metallic silver nanoparticles in a pilot wastewater treatment plant. *Environ. Sci. Technol.* **2011**, *45* (9), 3902−3908.
(13) Donner, E.; Scheckel, K.; Sekine, R.; Popelka-Filcoff, R. S.; Bennett, J. W.; Brunetti, G.; Naidu, R.; McGrath, S. P.; Lombi, E. Non-labile silver species in biosolids remain stable throughout 50 years of weathering and ageing. *Environ. Pollut.* **2015**, *205*, 78−86.
(14) Dobias, J.; Bernier-Latmani, R. Silver release from silver nanoparticles in natural waters. *Environ. Sci. Technol.* **2013**, *47* (9), 4140−4146.
(15) Tanaka, M.; Yamaji, Y.; Fukano, Y.; Shimada, K.; Ishibashi, J.-I.; Hirajima, T.; Sasaki, K.; Sawada, M.; Okibe, N. Biooxidation of gold-, silver-, and antimony-bearing highly refractory polymetallic sulfide concentrates, and its comparison with abiotic pretreatment techniques. *Geomicrobiol. J.* **2015**, *32* (6), 538−548.
(16) Xiu, Z.-m.; Zhang, Q.-b.; Puppala, H. L.; Colvin, V. L.; Alvarez, P. J. J. Negligible particle-specific antibacterial activity of silver nanoparticles. *Nano Lett.* **2012**, *12* (8), 4271−4275.
(17) Morones-Ramirez, J. R.; Winkler, J. A.; Spina, C. S.; Collins, J. J. Silver enhances antibiotic activity against Gram-negative *Bacteria*. *Sci. Transl. Med.* **2013**, *5* (190), 190ra81.
(18) Saulou, C.; Jamme, F.; Girbal, L.; Maranges, C.; Fourquaux, I.; Cocaign-Bousquet, M.; Dumas, P.; Mercier-Bonin, M. Synchrotron FTIR microspectroscopy of *Escherichia coli* at single-cell scale under silver-induced stress conditions. *Anal. Bioanal. Chem.* **2013**, *405* (8), 2685−2697.
(19) Arakawa, H.; Neault, J. F.; Tajmir-Riahi, H. A. Silver(I) complexes with DNA and RNA studied by Fourier transform infrared spectroscopy and capillary electrophoresis. *Biophys. J.* **2001**, *81* (3), 1580−7.
(20) Holt, K. B.; Bard, A. J. Interaction of silver(I) ions with the respiratory chain of *Escherichia coli*: an electrochemical and scanning electrochemical microscopy study of the antimicrobial mechanism of micromolar Ag+. *Biochemistry* **2005**, *44* (39), 13214−13223.
(21) Wakshlak, R. B.-K.; Pedahzur, R.; Avnir, D. Antibacterial activity of silver-killed bacteria: the "zombies" effect. *Sci. Rep.* **2015**, *5*, 9555.
(22) McKee, M. S.; Filser, J. Impacts of metal-based engineered nanomaterials on soil communities. *Environ. Sci.: Nano* **2016**, *3* (3), 506−533.
(23) Langdon, K. A.; McLaughlin, M. J.; Kirby, J. K.; Merrington, G. The effect of soil properties on the toxicity of silver to the soil nitrification process. *Environ. Toxicol. Chem.* **2014**, *33* (5), 1170−1178.
(24) Colman, B. P.; Arnaout, C. L.; Anciaux, S.; Gunsch, C. K.; Hochella, M. F., Jr; Kim, B.; Lowry, G. V.; McGill, B. M.; Reinsch, B. C.; Richardson, C. J.; Unrine, J. M.; Wright, J. P.; Yin, L.; Bernhardt, E. S. Low concentrations of silver nanoparticles in biosolids cause adverse ecosystem responses under realistic field scenario. *PLoS One* **2013**, *8* (2), e57189.
(25) Schlich, K.; Klawonn, T.; Terytze, K.; Hund-Rinke, K. Hazard assessment of a silver nanoparticle in soil applied via sewage sludge. *Environ. Sci. Eur.* **2013**, *25* (1), 17.
(26) McKenzie, N. J.; Coughlan, K. J.; Cresswell, H. P. *Soil physical measurements and interpretation for land evaluation*; CSIRO Publishing: Collingwood, Victoria, 2002.
(27) Jenkinson, D. S.; Powlson, D. S. The effects of biocidal treatments on metabolism in soil—V. *Soil Biol. Biochem.* **1976**, *8* (3), 209−213.
(28) Langdon, K. A.; McLaughlin, M. J.; Kirby, J. K.; Merrington, G. Influence of soil properties and soil leaching on the toxicity of ionic silver to plants. *Environ. Toxicol. Chem.* **2015**, *34* (11), 2503−2512.
(29) Broos, K.; Uyttebroek, M.; Mertens, J.; Smolders, E. A survey of symbiotic nitrogen fixation by white clover grown on metal contaminated soils. *Soil Biol. Biochem.* **2004**, *36* (4), 633−640.
(30) Campbell, C. D.; Chapman, S. J.; Cameron, C. M.; Davidson, M. S.; Potts, J. M. A Rapid Microtiter Plate Method To Measure Carbon Dioxide Evolved from Carbon Substrate Amendments so as To Determine the Physiological Profiles of Soil Microbial Communities by Using Whole Soil. *Appl. Environ. Microbiol.* **2003**, *69* (6), 3593−3599.
(31) Wakelin, S.; Lombi, E.; Donner, E.; MacDonald, L.; Black, A.; O'Callaghan, M. Application of MicroResp for soil ecotoxicology. *Environ. Pollut.* **2013**, *179*, 177−184.
(32) Bell, C. W.; Fricks, B. E.; Rocca, J. D.; Steinweg, J. M.; McMahon, S. K.; Wallenstein, M. D. High-throughput fluorometric measurement of potential soil extracellular enzyme activities. *J. Visualized Exp.* **2013**, DOI: 10.3791/50961.
(33) Niemi, R. M.; Vepsäläinen, M. Stability of the fluorogenic enzyme substrates and pH optima of enzyme activities in different Finnish soils. *J. Microbiol. Methods* **2005**, *60* (2), 195−205.
(34) Kreader, C. A. Relief of amplification inhibition in PCR with bovine serum albumin or T4 gene 32 protein. *Appl. Environ. Microbiol.* **1996**, *62* (3), 1102−1106.
(35) Hunter, N.; Nadkarni, M. A.; Martin, F. E.; Jacques, N. A. Determination of bacterial load by real-time PCR using a broad-range (universal) probe and primers set. *Microbiology* **2002**, *148* (1), 257−266.
(36) Fierer, N.; Jackson, J. A.; Vilgalys, R.; Jackson, R. B. Assessment of soil microbial community structure by use of taxon-specific quantitative PCR assays. *Appl. Environ. Microbiol.* **2005**, *71* (7), 4117−4120.
(37) DeLong, E. F. Archaea in coastal marine environments. *Proc. Natl. Acad. Sci. U. S. A.* **1992**, *89* (12), 5685−5689.
(38) Ritz, C.; Streibig, J. C., Bioassay Analysis using R. *J. Stat Softw* **2005**, *12*, (5); DOI. DOI: 10.18637/jss.v012.i05
(39) R Core Team. *R: A language and environment for statistical computing, reference index version* 3.3.3; R Foundation for Statistical Computing, 2017.
(40) Ritz, C.; Baty, F.; Streibig, J. C.; Gerhard, D. Dose-response analysis using R. *PLoS One* **2016**, *10* (12), e0146021.
(41) Spiess, A. N. *qpcR: Modelling and analysis of real-time PCR data*, 2014.
(42) Spiess, A. N.; Neumeyer, N. An evaluation of R(2)as an inadequate measure for nonlinear models in pharmacological and biochemical research: a Monte Carlo approach. *BMC Pharmacol.* **2010**, *10*, 6−6.
(43) Sunna, A.; Antranikian, G. Xylanolytic Enzymes from Fungi and Bacteria. *Crit. Rev. Biotechnol.* **1997**, *17* (1), 39−67.
(44) Lynd, L. R.; Weimer, P. J.; van Zyl, W. H.; Pretorius, I. S. Microbial Cellulose Utilization: Fundamentals and Biotechnology. *Microbiol Mol. Biol. Rev.* **2002**, *66* (3), 506−577.
(45) Burns, R. G.; DeForest, J. L.; Marxsen, J.; Sinsabaugh, R. L.; Stromberger, M. E.; Wallenstein, M. D.; Weintraub, M. N.; Zoppini, A. Soil enzymes in a changing environment: Current knowledge and future directions. *Soil Biol. Biochem.* **2013**, *58* (0), 216−234.
(46) Carroll, R. K.; Veillard, F.; Gagne, D. T.; Lindenmuth, J. M.; Poreba, M.; Drag, M.; Potempa, J.; Shaw, L. N. The Staphylococcus aureus leucine aminopeptidase LAP is localized to the bacterial cytosol and demonstrates a broad substrate range that extends beyond leucine. *Biol. Chem.* **2013**, *394* (6), 791−803.
(47) Matsui, M.; Fowler, J. H.; Walling, L. L. Leucine aminopeptidases: diversity in structure and function. *Biol. Chem.* **2006**, *387* (12), 1535−44.
(48) Caldwell, B. A. Enzyme activities as a component of soil biodiversity: A review. *Pedobiologia* **2005**, *49* (6), 637−644.
(49) Bell, R. A.; Kramer, J. R. Structural chemistry and geochemistry of silver-sulfur compounds: Critical review. *Environ. Toxicol. Chem.* **1999**, *18* (1), 9−22.
(50) Cregut, M.; Piutti, S.; Slezack-Deschaumes, S.; Benizri, E. Compartmentalization and regulation of arylsulfatase activities in Streptomyces sp., Microbacterium sp. and Rhodococcus sp. soil isolates in response to inorganic sulfate limitation. *Microbiol. Res.* **2013**, *168* (1), 12−21.
(51) Kertesz, M. A.; Leisinger, T.; Cook, A. M. Proteins induced by sulfate limitation in Escherichia coli, Pseudomonas putida, or Staphylococcus aureus. *J. Bacteriol.* **1993**, *175* (4), 1187−1190.

DOI: 10.1021/acs.est.8b00677
Environ. Sci. Technol. 2018, 52, 8745−8755

(52) Kendig, E. L.; Le, H. H.; Belcher, S. M. Defining Hormesis: Evaluation of a Complex Concentration Response Phenomenon. *Int. J. Toxicol.* **2010**, *29* (3), 235−246.
(53) Calabrese, E. J.; Baldwin, L. A. Defining hormesis. *Hum. Exp. Toxicol.* **2002**, *21* (2), 91−97.
(54) Doolette, C. L.; Gupta, V. V. S. R.; Lu, Y.; Payne, J. L.; Batstone, D. J.; Kirby, J. K.; Navarro, D. A.; McLaughlin, M. J. Quantifying the sensitivity of soil microbial communities to silver sulfide nanoparticles using metagenome sequencing. *PLoS One* **2016**, *11* (8), e0161979.
(55) Yang, Y.; Wang, J.; Xiu, Z.; Alvarez, P. J. J. Impacts of silver nanoparticles on cellular and transcriptional activity of nitrogen-cycling bacteria. *Environ. Toxicol. Chem.* **2013**, *32* (7), 1488−1494.
(56) Peyrot, C.; Wilkinson, K. J.; Desrosiers, M.; Sauvé, S. Effects of silver nanoparticles on soil enzyme activities with and without added organic matter. *Environ. Toxicol. Chem.* **2014**, *33* (1), 115−125.
(57) Smolders, E.; Oorts, K.; Sprang, P. V.; Schoeters, I.; Janssen, C. R.; McGrath, S. P.; Mclaughlin, M. J. Toxicity of trace metals in soil as affected by soil type and aging after contamination: using calibrated bioavailability models to set ecological soil standards. *Environ. Toxicol. Chem.* **2009**, *28* (8), 1633−1642.
(58) Wang, P.; Menzies, N. W.; Chen, H.; Yang, X.; McGrath, S. P.; Zhao, F.-J.; Kopittke, P. M. Risk of silver transfer from soil to the food chain is low after long-term (20 years) field applications of sewage sludge. *Environ. Sci. Technol.* **2018**, *52*, 4901.
(59) Klitzke, S.; Metreveli, G.; Peters, A.; Schaumann, G. E.; Lang, F. The fate of silver nanoparticles in soil solution — Sorption of solutes and aggregation. *Sci. Total Environ.* **2015**, *535*, 54−60.
(60) Sekine, R.; Khurana, K.; Vasilev, K.; Lombi, E.; Donner, E. Quantifying the adsorption of ionic silver and functionalized nanoparticles during ecotoxicity testing: test container effects and recommendations. *Nanotoxicology* **2015**, *9* (8), 1005−1012.
(61) Frankenberger, W. T.; Johanson, J. B. Effect of pH on enzyme stability in soils. *Soil Biol. Biochem.* **1982**, *14* (5), 433−437.
(62) Schlich, K.; Hund-Rinke, K. Influence of soil properties on the effect of silver nanomaterials on microbial activity in five soils. *Environ. Pollut.* **2015**, *196* (Suppl C), 321−330.

DOI: 10.1021/acs.est.8b00677
Environ. Sci. Technol. 2018, 52, 8745−8755